

EFFECT OF STIRRUP DIAMETER AND CONFIGURATION ON DIAGONAL COMPRESSIVE CAPACITY OF HSC BEAMS

Patarapol TANTIPIDOK^{*1}, Koji MATSUMOTO^{*2} and Junichiro NIWA^{*3}

ABSTRACT

This paper investigated the effect of stirrup diameter and configuration on the diagonal compressive capacity of HSC beams and compared the results with the prediction by the existing equations. Four 590-mm-depth I-beams were tested by three-point bending. As a result, the effect of stirrup diameter was insignificant. Even when wide stirrup spacing was used, a sufficient confinement effect was achieved by providing two-legged stirrups, and the localization of compressive stress was prevented. The existing equations should be improved in both accuracy and appropriateness.

Keywords: diagonal compressive capacity, high strength concrete, web crushing, stirrup spacing

1. INTRODUCTION

The combination of thin web (T- or I-shaped cross section) high strength concrete (HSC) beams and dense stirrups is one of the approaches used for economical and efficient design of concrete infrastructures. However, when excessive stirrups are provided, this combination will lead to diagonal compression failure, that is, an uncommon type of shear failure caused by the crushing of web concrete prior to stirrup yielding. The research on the mechanism of the diagonal compression failure is insufficient since it is usually avoided in design.

The standard specifications of JSCE [1] for the diagonal compressive capacity of reinforced concrete (RC) beams provide inadequate accuracy and limit the applicability to concrete with compressive strength (f'_c) up to 50 N/mm², resulting in extravagant and inefficient designs of RC beams. At present, only a few studies have been performed on the diagonal compressive capacity of HSC beams with the exception of recent research by the authors [2], [3]. The authors [2] concluded that the major factors affecting the diagonal compressive capacity were f'_c and stirrup spacing (s). The effect of shear-span to effective depth ratio (a/d), flange width to web width ratio (b_f/b_w) and effective depth (d) was found to have less influence in their study range. Subsequently, an accurate and simple predictive equation was proposed on the basis of the experiments [2]. However, the equation does not cover the application to RC beams with $s > 160$ mm, which can be occurred in the design of real structures. The effect of wide stirrup spacing ($s = 300, 370$ mm) was further investigated by the authors [3] and found to have a different tendency from the previous experiment [2]. It was pointed out that, in the case of HSC beams with wide stirrup spacing (s), stirrup configuration might

affect the diagonal compressive capacity and s might not be an appropriate indicator for the diagonal compressive capacity, but stirrup ratio (r_w).

The purpose of this research is to clarify the effect of stirrup diameter and configuration on the diagonal compressive capacity of relatively large RC beams with wide stirrup spacing, for promoting the rational design and more widespread use of HSC. The experiments of thin web HSC beams with wide stirrup spacing have been performed. Finally, the accuracy of the existing equations is verified. This research is a step forward toward the development of new design equation for the diagonal compressive capacity of RC beams, applicable to high strength concrete and wide stirrup spacing.

2. REVIEW OF THE EXISTING EQUATIONS FOR DIAGONAL COMPRESSIVE CAPACITY

2.1 The equation by the authors

The authors investigated the effect of f'_c , r_w , s , a/d , b_f/b_w and d on the diagonal compressive capacity and proposed a simple predictive equation based on the experimental results as the following [2]:

$$V_{cat} = (1.9 - \frac{s}{190})\sqrt{f'_c} b_w d \quad (1)$$

where; f'_c and s are in N/mm² and mm, respectively. The equation considers the equilibrium condition of web concrete at the critical section and assumes that the average distribution of diagonal compressive stress in the web and the member failure is caused by the crushing of web concrete without yielding of stirrup. The equation was empirically derived on the basis of the results that the diagonal compressive capacity linearly decreased with larger s regardless of its

*1 Ph. D. Candidate, Graduate School of Civil Engineering, Tokyo Institute of Technology, JCI Member

*2 Assistant Prof., Dept. of Civil Engineering, Tokyo Institute of Technology, Dr. E., JCI Member

*3 Prof., Dept. of Civil Engineering, Tokyo Institute of Technology, Dr. E., JCI Member

diameter and configuration. This is because insufficient confinement effects provided by stirrups caused the localization of compressive stress in struts. Thus, s was prominent, rather than r_w , for evaluating the diagonal compressive capacity in range of s from 45 mm to 160 mm. The effect of spacing became more significant with higher concrete strength; hence, the effect of f'_c and s was interrelated. On the other hand, the effect of a/d from 3.0 to 4.5, b_f/b_w from 3.75 to 12.5 and d from 220 mm to 319 mm had almost no influence on the diagonal compressive capacity of RC beams. The equation can be implemented to beams with f'_c : 19-165 N/mm², r_w : 0.6-4%, s : 45-165 mm, b_f/b_w : 3.75-12.5, a/d : 2.5-4.5 and d : 220-563 mm.

2.2 The equation by Placas and Regan

Placas and Regan proposed an empirical equation for evaluating the diagonal compressive capacity as the following [4]:

$$V_{Placas} = (1.04 + 0.21r_w)\sqrt{f'_c}b_wd \quad (2)$$

Factors involving the diagonal compressive capacity in this equation are f'_c (N/mm²) and stirrup ratio r_w (%). Although there is no upper limit of f'_c stated in this equation, the experimental evidences used to derive this equation approximates 35 N/mm².

2.3 JSCE Standard Specifications

In JSCE standard specifications [1], only f'_c (N/mm²) is considered as the influencing parameter of the diagonal compressive capacity. Because this formula was originally proposed for application to normal strength concrete, the equation is only valid for concrete with f'_c not exceeding 50 N/mm².

$$V_{JSCE} = 1.25\sqrt{f'_c}b_wd \quad (3)$$

3. EXPERIMENTAL PROGRAM

3.1 Specimen details

The experimental program prepared four RC beams with I-shaped cross section. Two specimens presented in previous research by the authors [3] were included for further discussion. Assuming no effect of d based on the previous result [2], d of the specimens in this research was greatly enlarged than in the previous one in order to provide wider s . Three-point bending tests were conducted by a 3000kN capacity loading apparatus. The summary of experimental cases and details of specimens are provided in Table 1 and Fig. 1, respectively. The main parameters were stirrup spacing ($s = 230, 300$ and 370 mm), stirrup diameter ($\phi_d = 13.1$ and 15.9 mm, $A_w = 125$ mm² and 198.6 mm²) and number of stirrup legs (one and two). The constant variables were the following: the web width (b_w) of 80

Table 1 List of the experimental cases

Specimen	f'_c [N/mm ²]	b_w [mm]	d [mm]	a [mm]	a/d	p_w^{*1} [%]	D^{*2} [mm]	Stirrup properties				
								ϕ_d^{*3} [mm]	f_{wy}^{*4} [N/mm ²]	No. of legs	r_w^{*5} [%]	s^{*6} [mm]
s300-II ^[3]	100	80	500	1500	3.0	8.9	22.2 (top)	13.1	1368	Two	1.06	300
s370-II(13) ^[3]											0.88	370
s370-II(16)							25.4 (bottom)	15.9	916	One	1.34	
s230-I											1.08	230

*¹ longitudinal reinforcement ratio ($=100A_s/(b_wd)$), *² nominal diameter of tensile bars, *³ nominal diameter of stirrups, *⁴ yield strength of stirrups, *⁵ stirrup ratio ($=100A_w/(b_ws)$), *⁶ spacing of stirrups

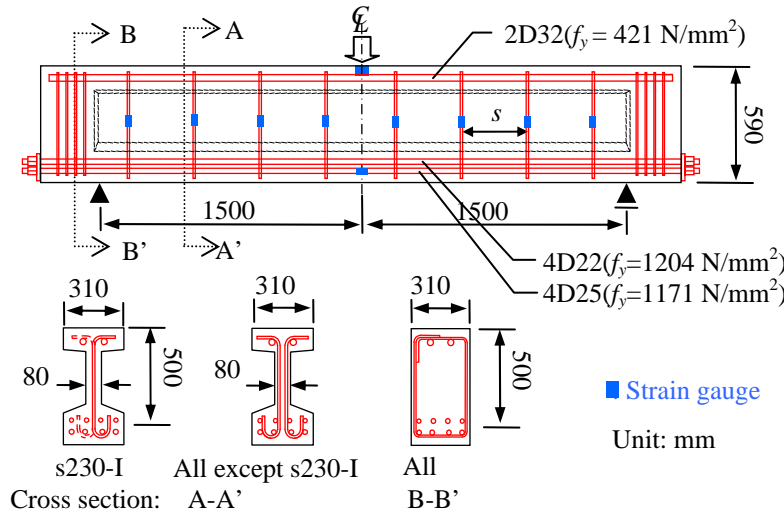


Fig. 1 Dimensions of specimens and layout of steel bars

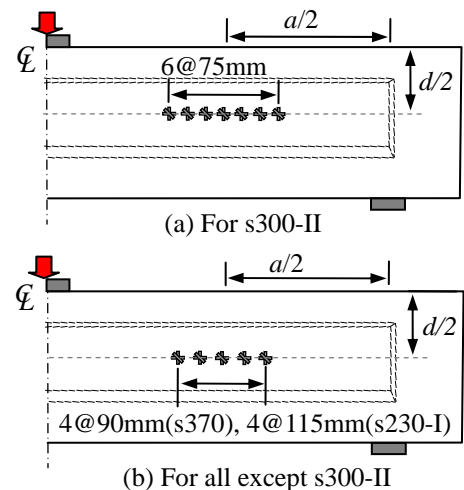


Fig. 2 Location of tri-axis strain gauges

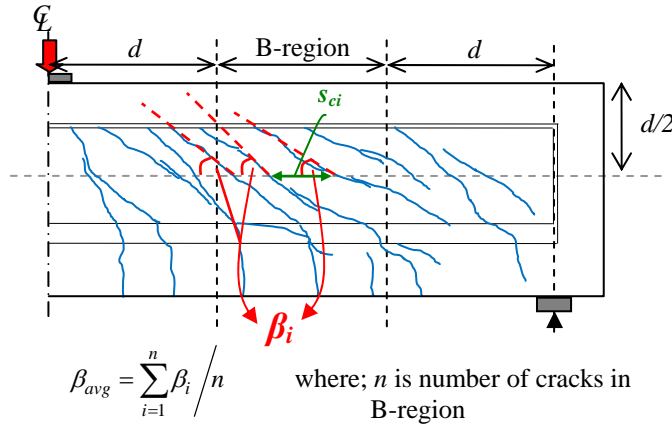


Fig. 3 Example of crack spacing and angle measurement

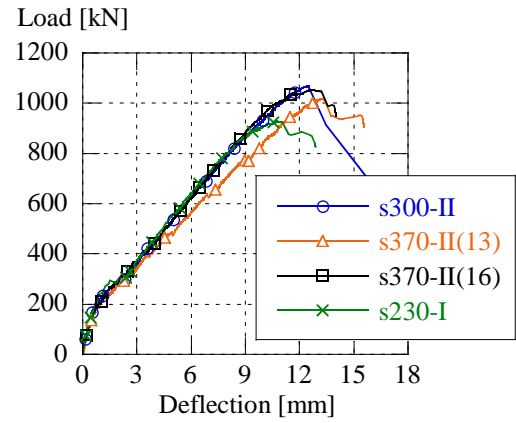


Fig. 4 Load-deflection relationship

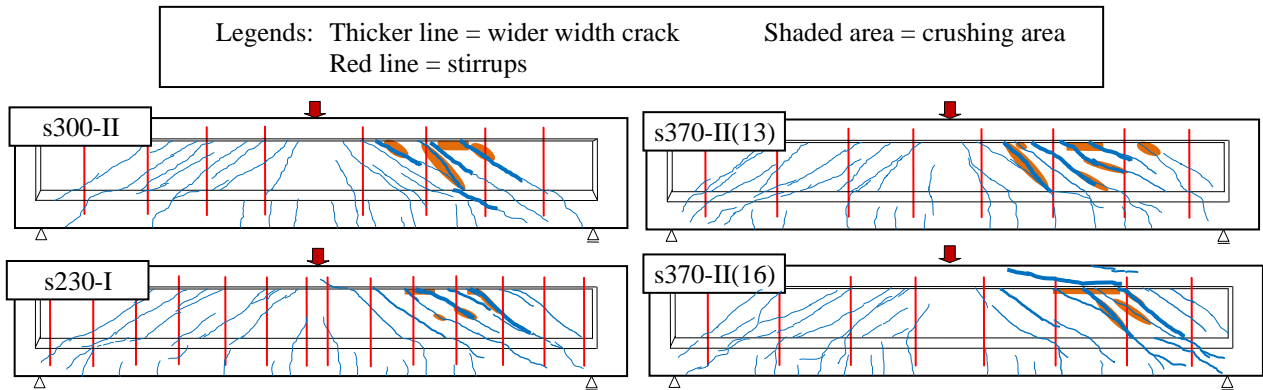


Fig. 5 Crack patterns just before the peak load

mm, the effective depth (d) of 500 mm, shear span (a) of 1500 mm, a/d of 3.0, longitudinal reinforcement ratio (p_w) of 8.9% and the total length of 3600 mm. Tensile reinforcements had two layers which D22 ($A_s = 380.1 \text{ mm}^2$) were used as top layer (Top) while bottom layer (Bottom) was D25 ($A_s = 490.9 \text{ mm}^2$). Compressive reinforcements were D32 ($A'_s = 804.2 \text{ mm}^2$). Stirrups were anchored around a tensile bar by the semi-circular hook type with 32.5 mm hook radius, and their straight extension was 80-88 mm.

All specimens were designed to be symmetric and be able to resist against the flexure failure and the diagonal tension failure by using high strength reinforcing bars as both of the tensile and shear reinforcements. In addition, the combination of thin web cross section and dense stirrups will cause specimens to exhibit the diagonal compression failure. In order to avoid the local failure, the web width outside support was increased to that of the bottom flange. Anchor plates and nuts were used to ensure the sufficient anchorage of the tensile bars and prevent anchorage failure.

3.2 Instrumentation and test procedures

For all specimens, applied load, mid-span deflections and strains of concrete, longitudinal bars and stirrups were measured. Concrete strain gauges were attached at the top fiber of the mid span. Strain gauges were attached at the mid span to measure the

strain of longitudinal bars whereas at the distance of $d/2$ from compression fiber for all stirrups in the shear spans. Angle of principle strain of web concrete was measured by tri-axis strain gauges. The locations of these strain gauges are illustrated in Fig. 2. Besides, surfaces of all specimens were painted by white color to ease the drawing and observing of cracks during the experiments. Pictures were taken by two digital single-lens reflex cameras for both shear spans. From the pictures taken at the peak load, the crack spacing in horizontal direction (s_{ci}) and the crack angle (β_i) were measured at the middle height of the web. The example of s_{ci} and β_i measurement of a crack is presented in Fig. 3. The average of s_{ci} of cracks in the shear span ($s_{c,avg}$) and the average of β_i of cracks in B-region (β_{avg}) will be used in the later discussion since it was observed that the crushing area, which is corresponding to the failure region, was mostly found in B-region (the portion outside the distance approximately d away from the loading point and supports).

4. EXPERIMENTAL RESULTS

4.1 Load-deflection relationship

Load-deflection relationships are illustrated in Fig. 4. Firstly, specimens behaved in elastic manner until the first flexural crack occurred in the bottom flange near the mid span, which is reflected in the graph as a rate of inclination decreases. After the first flexural

Table 2 Experimental results

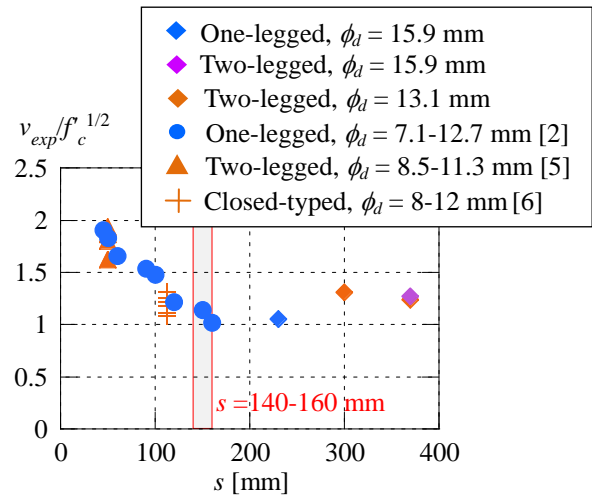
Specimen	f_c' [N/mm ²]	d [mm]	a/d	r_w [%]	s [mm]	ϕ_d [mm]	No. of stirrup legs	f_y [N/mm ²]	$\sigma_{s, \max}^{*1}$ [N/mm ²]	f_{wy} [N/mm ²]	$\sigma_{w, \max}^{*2}$ [N/mm ²]	$s_{c, avg}^{*3}$ [mm]	β_{avg}^{*4} [°]	V_{exp}^{*5} [kN]
s300-II	104	500	3.0	1.1	300	13.1	Two	1171	400.8	1368	883	121.6	36.0	535.0
s370-II(13)	105			0.9	370				724.4		904.8	144.9	33.7	508.5
s370-II(16)	102			1.3		15.9			297.6	926	731.8	164.5	33.3	527.0
s230-I	123			1.1	230		One		515.2	916	809.0	155.9	36.8	465.0
C1.2-s150 ^[2]	105	220		1.2	150	9.53	One	1204	401.4	953	550.8	91.0	38.8	102.7
C1.5-s120 ^[2]	101			1.5	120				454.2		403.4	99.0	40.5	108.0
C1.8-s100 ^[2]	107			1.8	100				613.2		549.6	92.5	36.7	134.3
C2-s90 ^[2]	102			2.0	90	12.7		1198	601.0	954	561.2	69.9	31.0	137.0
C2-s50 ^[2]	110				50				765.0	721.0	60.0	36.5	168.5	
C2-s160 ^[2]	115				160				7.1	1214	420.6	955	300.8	86.0
C3-s60 ^[2]	98.2			3.0	60	9.53		1198	700.0	954	538.6	-	-	144.9
C4-s45 ^[2]	99.1			4.0	45				724.6		372.8	56.5	33.0	167.6
C-s100L ^[2]	108			319		2.2		100	12.7		1187	641.6	931	627.2

*¹ maximum stress in tensile bars, *² maximum stress in stirrups, *³ average crack spacing in horizontal direction at peak load, *⁴ average crack angle in B-region at peak load, *⁵ diagonal compressive capacity

crack, the load-deflection curve remained to advance almost linearly with the continuous initiation of diagonal cracks at the web concrete. Near the peak load, the deflection increased with a relatively small increase in applied load as the web concrete began to crush. Afterwards, the applied load reached to the peak. After the peak load, the applied load rapidly decreased. Data of the strains of longitudinal bars and stirrups revealed no yielding at the peak load. It implies that the failure mode was neither the flexure failure nor the diagonal tension failure. The web concrete crushed at the peak load and splitting cracks along the member axis near tensile bars did not initiate at that time; hence, the cause of failure was not by the anchorage failure of both tensile bars and stirrups. It can be concluded by considering these observations that the failure mode of all specimens was designated as the diagonal compression failure. The diagonal compression failure in which the web concrete crushed before the yielding of stirrup exhibited the brittle mode. Crack patterns just before the peak load are demonstrated in Fig. 5. The thicker lines and the shaded areas represent the wider width crack and the crushing areas, respectively. The experimental results including those in the previous study [2] are summarized in Table 2.

4.2 Effect of stirrup

The authors [2] adopted a method to eliminate the variation of f'_c by normalizing the obtained shear capacities ($v_{exp} = V_{exp}/(b_w d)$) by $f'_c{}^{1/2}$ which is used in the design equation of JSCE [1] and the predictive equation by Placas et al. [4]. This method is also applied in this study. The relationships between s and $v_{exp}/f'_c{}^{1/2}$ including the specimens in the study by the authors [2], Rangan [5] and Leonhardt et al. [6] are demonstrated in Fig. 6. The details of specimens by Rangan [5] and Leonhardt et al. [6] are provided in Table 3. From Fig. 6, considering the range of $s = 45-160$ mm, the

Fig. 6 Effect of s

diagonal compressive capacity has a linear relationship with s regardless of its diameters and configuration. On the contrary, the different tendency of the diagonal compressive capacity in the case of relatively wider s is observed according to the results in this study. Fig. 6 demonstrates that the change of $v_{exp}/f'_c{}^{1/2}$ becomes negligible when s is wider than approximately 140-160 mm. Specimens with same s but different ϕ_d (s370-II(13) and s370-II(16)) also have slight difference in the diagonal compressive capacity, confirming the conclusion by the authors [2] that the diameter of stirrup does not affect the diagonal compressive capacity. Furthermore, s230-I has lower diagonal compressive capacity than those of the others even its s is narrower. This is caused by the difference in the number of stirrup legs among these specimens. It will be explained in the following part.

Previous study [2] concluded that the reduction of the diagonal compressive capacity with the increase

in stirrup spacing is resulted from two mechanisms caused by the confinement effect by stirrups. One is smaller diagonal crack width (w) caused by providing closer shear reinforcements; therefore, the critical average stress in web concrete (σ_{2max}) would be greater. The other is the localization of compressive strut, which resulted from an insufficient confinement effect provided by stirrups. It is because the presence of confinement effect by stirrups can prevent the excessive crack opening so that the stress can distribute along the beam axis. Moreover, the research by the authors [2] indicated that in case of the closer-spacing specimens, cracks distribute more finely and the crushing area at web distributes more widely than that of the wider-spacing specimens. As well, $s_{c,avg}$ shows a decreasing trend with closer stirrup spacing and it is implied that the failure localization occurs when wider $s_{c,avg}$ is observed [2]. Zakaria et al. [7] reported that larger beams cause greater diagonal crack spacing and the authors [3] indicated that the crack spacing increases proportionally with the increase in d .

However, in this research, even though s was greatly increased, the diagonal compressive capacity did not decrease when using two-legged stirrups (s300-II, s370-II(13) and s370-II(16)) compared to s230-I. As for the case of two-legged stirrups, cracks were finely distributed and the crushing area at web was widespread as can be observed from Fig. 5. Considered from the previous research that $s_{c,avg}$ should be proportional to the increase of s and d , $s_{c,avg}$ of the cases were relatively narrow. In addition, comparing specimens with the same r_w but different s , ϕ_d and number of legs (s230-I and s300-II), higher diagonal compressive capacity and smaller $s_{c,avg}$ (finer cracks distribution) were observed for s300-II even s230-I had narrower s and larger ϕ_d . This is because one-legged stirrup was provided in s230-I. From these evidences, it is confirmed that the confinement effect by stirrups was sufficient in the case of two-legged stirrups and the diagonal stress did not concentrate in a local area of the specimens even wide stirrup spacing was used. The use of two-legged stirrups of $\phi_d = 13.1$ mm resulted in a higher effective area in which the confinement effect (due to the stirrup) can control excessive crack opening, while the use of one-legged stirrup, for which the effective area was comparatively smaller, induced the localization of compressive strut.

4.3 Angle of diagonal cracks and principal strain

The measurement of angle of diagonal cracks was focused in B-region since it was observed that the crushing areas, which are corresponding to the failure regions, were mostly found in that region. In the previous research [2], a clear tendency of β_{avg} and each possible factor influencing the crack angle cannot be found. β_{avg} was varied from 27 to 47 degrees and the average values β_{avg} for all specimens was 36.6 degrees. From Table 2, β_{avg} of s300-II, s370-II(13), s370-II(16) and s230-I were 36.0, 33.7, 33.3 and 36.8 degrees, respectively. These values correspond to those observed in the previous experiment [2].

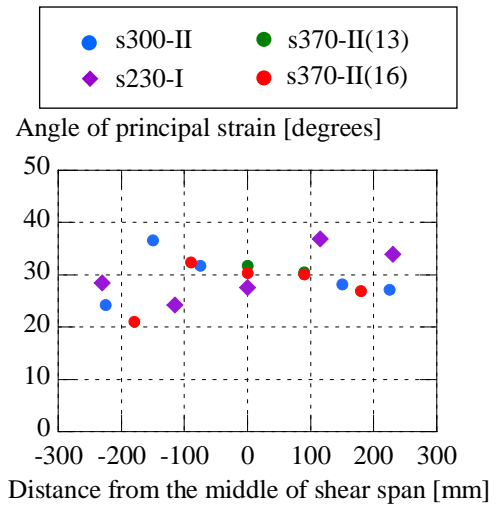


Fig. 7 Distribution of angle of principal strain

As for the angle of principal strain, the measured results at the peak load are exhibited in Fig. 7. The location of the measurement was shown in Fig. 2. Some gauges were broken during the experiments. The angle of principal strain varies from 21.3 to 36.9 degrees. The average angle of principal strain of s300-II, s370-II(13), s370-II(16) and s230-I are 29.6, 31.2, 28.2 and 30.3 degrees, respectively. As well, the angle of principal strain has no tendency with stirrup ratio, spacing, diameters and configuration.

5. COMPARISON WITH THE EQUATIONS

Table 3 presents a comparison of test results including those obtained by the authors [2], Rangan [5] and Leonhardt et al. [6] and the results calculated using the equations reviewed in chapter 2. The average of these ratios ($avg.$) with a coefficient of variation ($C.V.$) is also provided in Table 3. Placas equation (Eq. (2)) indicates an average of 0.99 with a $C.V.$ of 14.1 %. It implies that Eq. (2) can evaluate an average value with large variation. JSCE standard specifications (Eq. (3)) demonstrates the average of $V_{exp}/V_{JSCE} = 1.17$. The equation may be intended to be conservative because of safety reasons. Also, Eq. (3) gives larger variation ($C.V. = 20.3\%$) than Eq. (2).

Considering only the cases of wide stirrup spacing (s300-II, s370-II(13), s370-II(16), s230-I), the equation by Placas et al. (Eq. (2)) and JSCE equation (Eq. (3)) are accidentally accurate ($avg. = 0.96$ and 0.98 , $C.V. = 9.6\%$ and 9.7%). On the contrary, the equation by the authors (Eq. (1)) is inaccurate. This is an expected outcome since Eq. (1) is an empirical equation which may not be applicable outside of its application range. Within its range of application, the authors' equation gives a precise prediction ($avg. = 1.02$, $C.V. = 9.9\%$).

In conclusion, the existing equations should be improved in both accuracy and appropriateness since Eq. (1) has limited applicable range, Eq. (2) considers r_w as a representative of the effect of stirrup which

Table 3 Comparison between the experiment and calculated results

Specimen	f'_c [N/mm ²]	b_w [mm]	d [mm]	a/d	r_w [%]	ϕ_d [mm]	s [mm]	Stirrup Configuration	$V_{exp}/$ V_{cal}	$V_{exp}/$ V_{Placas}	$V_{exp}/$ V_{JSCE}	
s300-II	104	80	500	3.0	1.1	13.1	300	Two-legged	-	1.04	1.05	
s370-II(13)	105				0.9		370		-	1.01	0.99	
s370-II(16)	102				1.3	15.9			-	0.97	1.03	
s230-I	123							1.1		230		-
C1.2-s150 ^[2]	105	40	220		1.2	9.53	150	One-legged	1.03	0.84	0.91	
C1.5-s120 ^[2]	101				1.5		120		0.96	0.86	0.98	
C1.8-s100 ^[2]	107				1.8		100		1.07	0.99	1.18	
C2-s90 ^[2]	102				2.0		90		1.08	1.00	1.23	
C2-s50 ^[2]	110				2.0	50	1.12		1.19	1.46		
C2-s160 ^[2]	115				2.0	12.7	160		0.97	0.67	0.88	
C3-s60 ^[2]	98.2				3.0	9.53	60		1.05	0.95	1.33	
C4-s45 ^[2]	99.1				4.0		45		1.15	0.97	1.53	
C-s100L ^[2]	108								2.2	12.7	100	
I1 ^[5]	36.5	74	563	2.5	2.7	11.3	50	Two-legged	1.10	1.12	1.44	
I2 ^[5]	30.2				1.5	8.5			0.99	1.2	1.3	
I3 ^[5]	31.2				63	3.2			11.3	1.14	1.09	1.49
I4 ^[5]	35.7				64	1.8			8.5	1.18	1.36	1.55
TA1 ^[6]	20.6	150	375	3.3	1.3	12	113	Closed-type	1.01	1.00	1.05	
TA2 ^[6]	20.6				0.9	10			0.9	0.97	0.94	
TA3 ^[6]	19.1				0.6	8			0.85	0.95	0.88	
TA13 ^[6]	23.7				1.3	12			0.96	0.96	1.00	
TA14 ^[6]	23.7				0.9	10			0.93	1.00	0.97	
TA15 ^[6]	23.2				0.6	8			0.83	0.93	0.86	

*: Except for s300-II, s370-II(13), s370-II(16), s230-I because out of applicable range

avg. 1.02* 0.99 1.17
C.V. 9.9%* 14.1% 20.3%

contrasts to the reported insignificant effect of stirrup diameter in this study, and Eq. (3) does not consider the effect of stirrup. Further research regarding these matters is required.

6. CONCLUSIONS

The experiments with thin web and high strength concrete beams with wide stirrup spacing have been preformed. The research is a step in the direction to the development of rational designs for the diagonal compressive capacity of reinforced concrete beams. As a result, the diagonal compressive capacity linearly decreases with wider stirrup spacing regardless of its diameters and configuration when stirrup spacing is narrower than 140 mm. On the other hand, when stirrup spacing is wider than approximately 140-160 mm, the effect of spacing becomes negligible as well as the diameter. Even wide stirrup spacing is provided, the use of two-legged stirrup results in the relatively finer distribution of cracks, the more widespread distribution of crushing area at web and the narrower average crack spacing in horizontal direction compared to specimens with one-legged stirrup. A sufficient confinement effect is achieved by providing two-legged stirrups, and the localization of compressive stress in struts can be prevented. The existing equations should be improved in both accuracy and appropriateness.

REFERENCES

- [1] Japan Society of Civil Engineers (JSCE), "Standard Specifications for Concrete Structures-2007, Design," 2007
- [2] Tantipidok, P. et al., "Proposed Predictive Equations for Diagonal Compressive Capacity of Reinforced Concrete Beams," Journal of Japan Society of Civil Engineers, Ser. E2 (Materials and Concrete Structures), Vol. 67, No. 4, 2011, pp. 535-548.
- [3] Tantipidok, P., Matsumoto, K. and Niwa, J., "The Effect of Wide Stirrup Spacing on Diagonal Compressive Capacity of High Strength Concrete Beams," Proceedings of the Japan Concrete Institute, Vol. 34, Jul. 2012, pp. 487-492
- [4] Placas, A. and Regan, P. E., "Shear Failure of Reinforced Concrete Beam", ACI Journal, Vol. 68, No. 10, 1971, pp. 763-774.
- [5] Rangan, B. V., "Web Crushing Strength of Reinforced and Prestressed Concrete Beams," ACI Structural Journal, Vol. 88, 1991, pp. 12-16.
- [6] Leonhardt, F. and Walther, R., "Shear Tests on T-Beam with Varying Shear Reinforcement," Deutscher Ausschuss für Stahlbeton, No. 156, 1963, pp. 1-84.
- [7] Zakaria, M. et al., "Experimental Investigation on Shear Cracking Behavior in Reinforced Concrete Beams with Shear Reinforcement", Journal of Advanced Concrete Technology, Vol. 7, No. 1, Feb. 2009, pp. 79-96.